TECHNICAL MEMORANDUM

589

4D-Var Assimilation of MERIS Total Column Water Vapour Retrievals over Land

Peter Bauer

Research Department

European Centre for Medium-Range Weather Forecasts, UK

Submitted for publication in QJRMS

April 2009

European Centre for Medium-Range Weather Forecasts
Europäisches Zentrum für mittelfristige Wettervorhersage
Centre européen pour les prévisions météorologiques à moyen terme

Series: ECMWF Technical Memoranda

A full list of ECMWF Publications can be found on our web site under:
http://www.ecmwf.int/publications/

Contact: library@ecmwf.int

Abstract

Experiments with the active assimilation of total column water vapour retrievals from Envisat MERIS observations have been performed at ECMWF focusing for the summer 2006 AMMA field campaign period. A mechanism for data quality control, observation error definition and variational bias correction have been developed so that the data can be safely treated within 4D-Var like other observations that are currently assimilated in the operational system. While data density is limited due to its restriction to daylight and cloud-free conditions, a systematic impact on mean moisture analysis was found with distinct regional and seasonal features. The impact can last 1-2 days into the forecast but has little impact on forecast accuracy both in terms of moisture and dynamics. This is mainly explained by the weak dynamic activity in the areas of largest data impact. Evaluation with radiosonde observations revealed a strong dependence on radiosonde type. Compared to Vaisala RS92 observations, the addition of MERIS total column water vapour observations produced neutral to positive impact while contradictory results were obtained when all radiosonde types were used in generating the statistics. This highlights the issue of radiosonde moisture biases and the importance of sonde bias correction in NWP.

1 Introduction

Satellite observation of moisture over land surfaces requires the distinction between signal contributions from the surface and those from the atmosphere. Since most of the atmospheric moisture is available in the lower levels, the surface contribution to radiances measured at the top of the atmosphere is large. The accurate modeling of surface emission requires knowledge of surface emissivity and surface skin temperature. Surface emission largely depends on soil type, condition (e.g. wet or dry), coverage and, depending on wavelength, can undergo large diurnal and regional variations. In radiometric terms, skin temperature relates to the physical temperature of the surface layer most of the radiation is emitted from, which may be the thinnest top-layer of the surface for infrared wavelengths or deeper layers for microwaves.

Due to the difficulties associated with the radiative transfer modeling of surface emission for radiance data only radiometer channels with little surface contribution are assimilated at ECMWF and most other Numerical Weather Prediction (NWP) centres. Tight first-guess departure checks are applied to the active radiometer channels to avoid aliasing erroneous surface emission estimates into atmospheric increments. For moisture over land surfaces, only Advanced Microwave Sounding Unit (AMSU-B) and Microwave Humidity Sounder (MHS) channels 3-4 are actively assimilated and with considerable data gaps where surface emission is considered uncertain. Improvement is expected from methods dynamically deriving surface emissivity directly from window channel observations and model skin temperature and using the derived emission for sounding channels (Karbou et al. 2006, Krzeminski et al. 2008, Karbou et al. 2009a, b).

Alternatively, active satellite data from water vapour lidars or visible/near-infrared radiometer data may be used if the instrument channel selection allows for differential absorption techniques to be applied. This technique uses the difference of radiance measurements between neighboring wavelengths of which one is located in a water vapour absorption band and the other in a window. Assuming that the surface constribution varies much weaker over the covered wavelength range, surface and atmospheric constributions can be distinguished. While water vapour differential absorption lidars have only reached demonstration stage, a few radiometers are actually in space which allow the application of differential absorption methods, namely the Medium Resolution Imaging Spectrometer (MERIS) onboard ESA's Envisat and the Global Ozone Monitoring Experiment-2 (GOME-2) onboard EUMETSAT's Metop satellites.

This paper summarizes the results from the implementation of MERIS total column water (TCWV) retrievals in the ECMWF 4D-Var data assimilation system. The technical implementation, the choices made for observation sampling, quality control, error definition and bias correction are described in Section 2. Results from the analysis and forecast evluation are presented in Section 3 and set into context with independent observational data due to the limited availability of operationally available verification in those geographical areas where the MERIS data produces the largest impact. The paper's conclusions are produced in Section 4.

2 MERIS observations

MERIS is a medium-resolution radiometer with 15 channels and programmable bandwidths in the visible and near-infrared spectral range between 390 nm and 1,040 nm. Spatial resolution of the radiance observations is 1,040 m x 1,200 m over oceans and 260 m x 300 m over land with a swath width of 1,150 km which provides global coverage over a period of 3 days. The level-2 product that is received at ECMWF in near-real time has a coverage of 1,150 km x 17,500 km and is resampled by ESA onto a "pseudo satellite" projection along the satellite track with a spatial resolution of 4.8 km x 4.8 km. Apart from the retrieved TCWV, the product contains cloud optical depth and cloud top height, mean sea-level pressure, wind speed, and information on solar and observation geometry. The expected accuracy of the main level-2 products is 10% for cloud optical depth and 20% for TCWV. The data has been received at ECMWF with several algorithm updates of which only the latest version is considered in this study that has been available since 2005.

The retrieval of TCWV is based on the differential absorption of reflected solar radiation in two narrow-band (10 nm wide) channels at 890 and 900 nm in the vicinity of a water vapour absorption line near 1μm (Bennartz and Fischer 2001). Variations of surface bidirectional reflectance can be assumed negligible across this spectral range and, over land surfaces, the magnitude of surface reflectance is sufficiently large to ensure a good signal-to-noise ratio. This data is therefore only available during local daytime and will only be used over land surfaces in this study.

As part of an ESA-contract, MERIS TCWV is also monitored at ECMWF outside the operational system. For this purpose, Abdalla (2005) has introduced a spatial averaging operator and additional quality control indicators related to the spatial statistical significance of MERIS retrievals. Abdalla investigated global comparison statistics noting general issues with the observational product over oceans and the fact that various geographical regions were found to be affected by systematic moisture differences. In the present paper, the observations have been channeled through the operational data handling system though and they were treated like all other satellite observations that are actively assimilated.

Experiments over various periods and with different model cycles have been run to test the set-up and to assess the impact of MERIS TCWV observations. Here, only results from the latest version will be presented because this version respresents the future operational configuration of model cycle 35R3 that includes the variational bias correction for TCWV observations. A three month experiment over the period July-September 2006 has been run to cover the African Monsoon Multidisciplinary Analyses (AMMA) during which a field campaign was performed in North-West Africa. In the course of the AMMA field campaigns additional ground-based observations of TCWV have been made available which will be added to the evaluation presented in this paper at a later stage (see discussion in Section 4).

The model experiments have been run at 40 km spatial resolution (T511) and with 91 model levels in a 12-hour 4D-Var configuration including the operational observing system that was available in summer 2006. The MERIS TCWV observation sample size is about 800-1,000 observations per analysis. The data has been sub-sampled to 0.5^o x 0.5^o to avoid spatial correlation and to reduce data amount. Another benefit from this is that observation sampling becomes more compatible with the model resolution of $\approx$40 km used in the non-linear trajectory calculations and of 250, 150, and 100 km used in the three inner loops of the 4D-Var minimization, respectively.

2.1 Screening and bias correction

In the subsequent analysis, only TCWV retrievals over land were employed in the absence of clouds. A first cloud screening was applied based on the MERIS-derived cloud optical depth product that is part of the TCWV product. However, TCWV biases remained between ECMWF model predictions and MERIS retrievals in the vicinity of clouds so that another screening based on model clouds was applied. While model clouds are not expected to be perfectly located, this two-step screening using both observed and modelled clouds ensures the assimilation of a safer product since model clouds with small liquid water contents tend to appear over larger areas than actually observed.

When TCWV departures between model first-guess and observations (FG-departures) are analyzed with respect to possible error sources, it was found that FG-departures are large for instrument scan angles above 35 degrees, possibly related to the instrument's viewing conditions onboard the satellite. These were therefore excluded from the subsequent analysis. No systematic problem could be found in FG-departures as a function of reflection angle that is the angle between sun and satellite instrument measured in the reflection plane.

Figure 1 shows the dependence of FG-departures on the above, namely scan-angle, ρ_{scan}, and reflection angle, ρ_{refl}, as well as TCWV. The latter indicates a small but systematic air-mass dependent bias that can be corrected as part of a bias-correction procedure. Initially, this was derived through a static regression-type correction based on TCWV as the only predictor. With model cycle 35R3 this will be treated as part of the variational bias correction scheme that is currently only applied to radiances at ECMWF (Dee 2005, Auligné et al. 2007). The data shown in Fig. 1c is already bias-corrected. The dashed line shows the fit to the small mean remaining bias indicating a successful bias correction.

Figure 2 shows the evolution of the first-guess and analysis departures as well as the bias correction over the experiment's period in the Northern hemisphere. Obviously, the data samples are rather low due to the fact that these observations are only available during daytime and in cloud-free conditions. This produces weakly noisy statistics. However, in the Northern hemisphere where most observations are available the bias correction performs well and produces nearly bias-free departures with bias corrections slightly larger than 0.5 kgm^{-2}. Note that the bias correction needs about 1 month to spin up. The results for the Tropics and Southern hemisphere are similar and are not shown here.

Lastly, as part of the data screening a FG-departure threshold check of 8 kg/m^2 was applied to avoid outliers. After quality control, FG-departure standard deviations were found to be around 2.5 kg/m^2.

Figure 3 shows the distribution of the observations that were actively assimilated in August 2006. Mean first-guess departures are rather small given the above described strict quality control. There are, however, a few local extremes, for example near the equator in both Africa and South America (Fig. 3b). These originate, however, from very small samples (Fig. 3c).

2.2 Observation errors

The remaining ingredient for assimilating the TCWV retrievals is the observation error. Bennartz and Fischer (2001) found an error standard deviation of 2.5 kg/m^2 when comparing the satellite retrievals to co-located radiosondes. This corresponds well to our FG-departures. Given the nature of TCWV error distribution a relative error seems more appropriate than an absolute error measure and therefore an independent error analysis was performed. As already used for TCWV obtained from 1D-Var retrievals of SSM/I radiances in clouds and precipitation (Bauer et al. 2006), the observation error was derived from the spatial covariance statistics of first-guess departures following the Hollingsworth and Loennberg (1986) method.

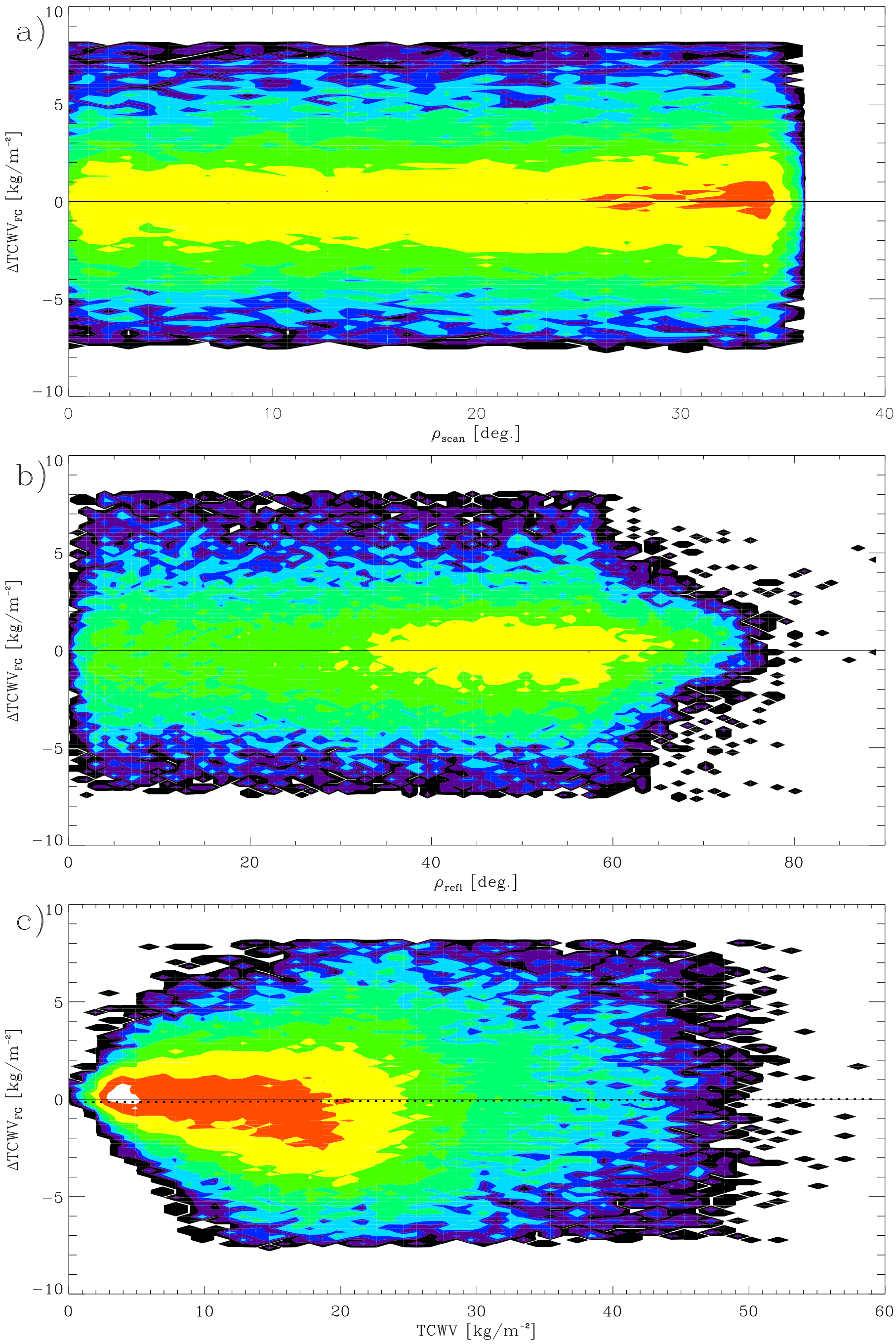

Figure 1: Histograms of first-guess departures as a function of scan-angle (a), reflection angle (b) and TCWV (c). Dashed line indicates linear fit to remaining bias. Data from August 2006 with sample size of 53,000. Colours denote data density with small values in blue and large values in red.

This method is based on the assumption that the observations are spatially uncorrelated so that, if spatial covariances are plotted as a function of observation separation distance, d, the values for $d > 0$ only contain background contributions while at $d = 0$ the values are composed of the sum of background and observation contributions. This allows the separation of the two contributions and leads to an error estimate of about 15% in

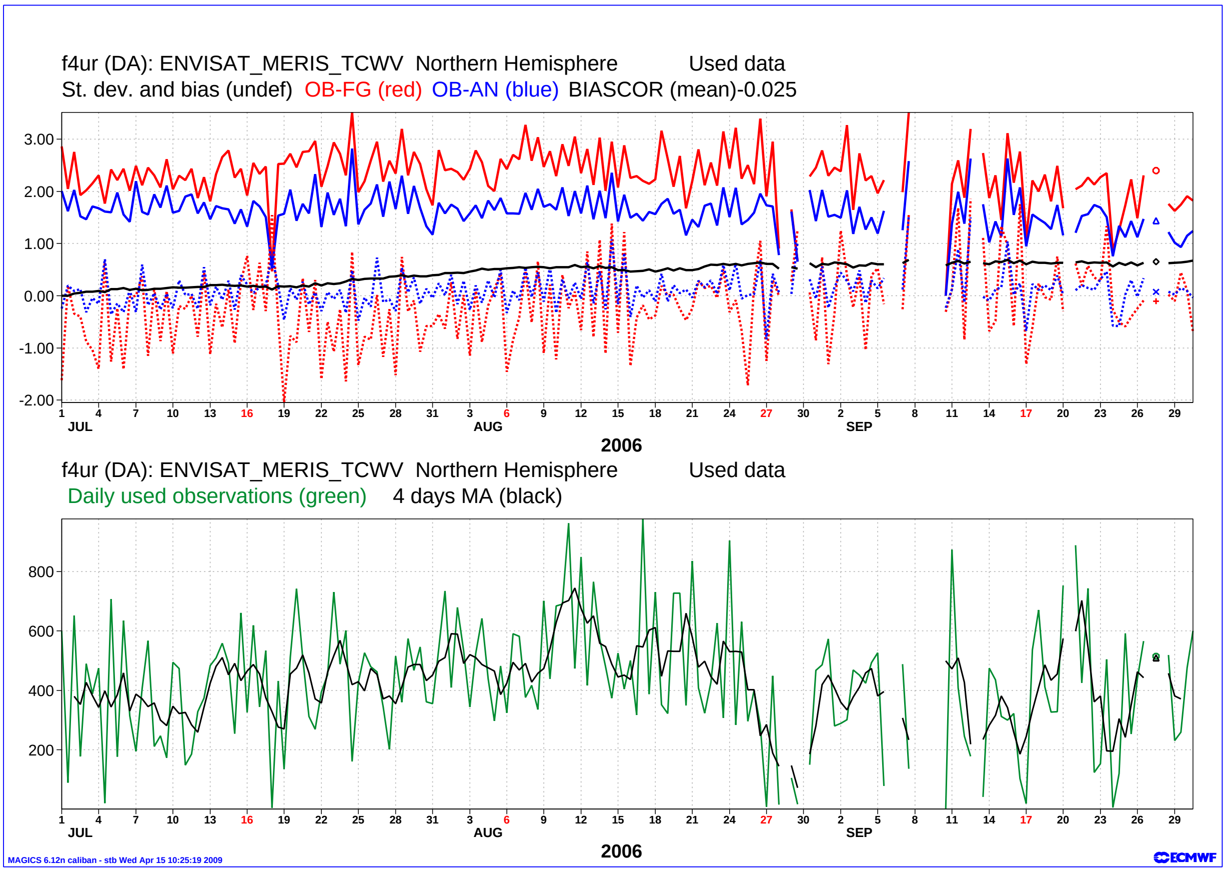

Figure 2: Top panel: Time series of TCWV first-guess (red) and analysis (blue) departure standard deviations (solid) and mean departures (dotted) as well as bias correction (black) in the Northern hemisphere. Bottom panel: daily observation counts (green) and 4-day averages (black).

our data sample (see Figure 4). These errors combine retrieval and interpolation errors. The latter stems from the interpolation of model grid-point TCWV to observation location and is part of the representativeness error.

3 Impact

As mentioned before, several impact experiments have been run for 2006, 2007 and 2008 but only the one that includes the variational bias correction will be presented here in detail. The experiment was run as a T511L91 12-hour 4D-Var experiment and initialized with the operational model/data. The variational bias correction was initialized with zero coefficients and only the model's first-guess TCWV serves as a bias predictor. As described in Section 2.1, the bias correction requires about 1 month of spin-up so that the evaluation will focus on the last two months of the experiments that is August-September 2006. A control experiment has been run with the identical set-up as the MERIS experiment except for the active assimilation of the data.

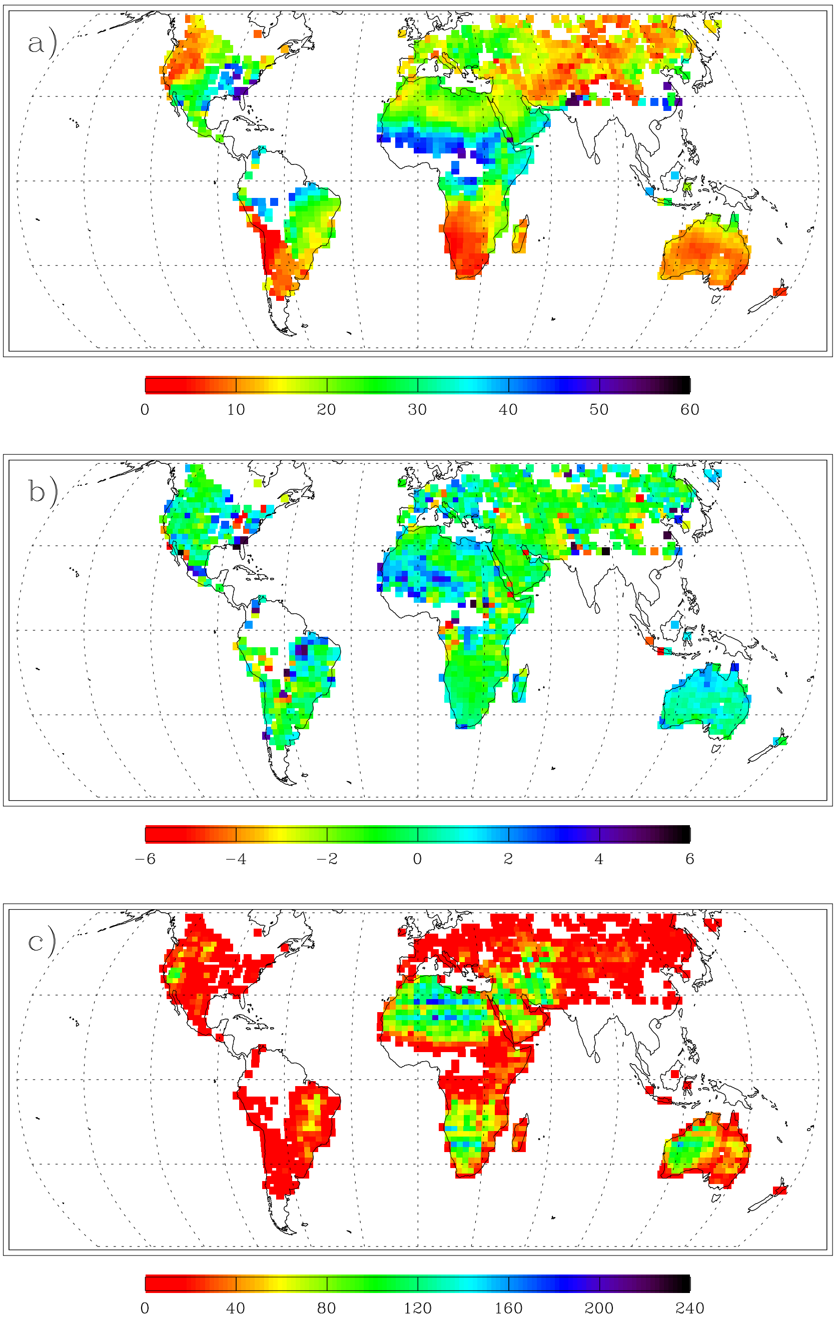

Figure 3: Mean observed TCWV (a, units kg/m^2), mean first-guess departures (b, units K) and sample size per 2.8 degree grid-box (c). Data from August 2006 with sample size of 53,000.

3.1 Mean fields

Figure 5a shows the mean TCWV analysis field from the control experiment's analysis and the difference between MERIS and control analyses (Figure 5b), the 1-day and 3-day forecasts (Figure 5c and d). The plots focus on those areas of the globe where the largest impact on the moisture analysis has been observed. Note

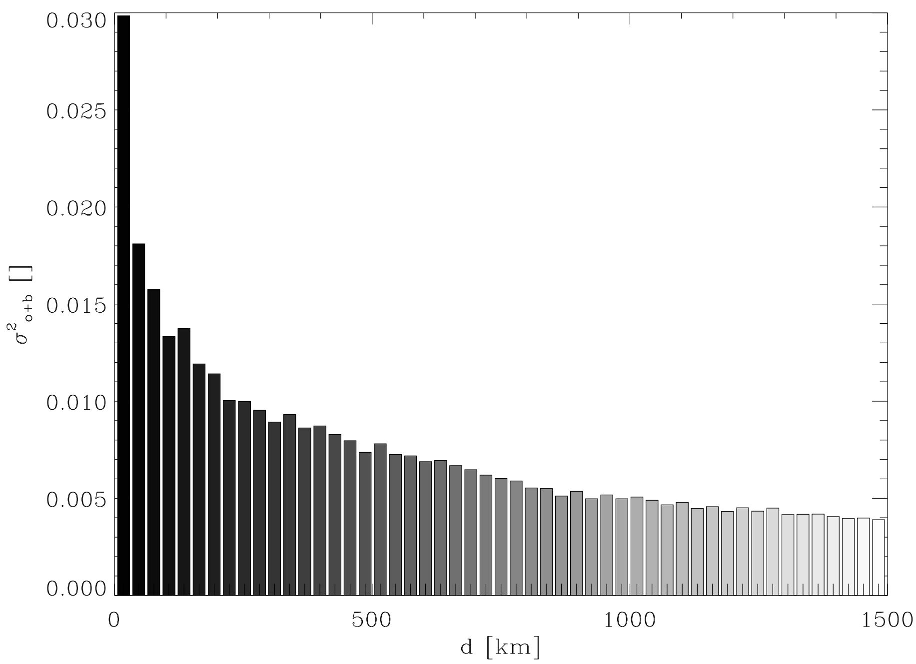

Figure 4: TCWV first-guess departure covariance as a function of separation distance.

that the difference plots refer to relative TCWV mean analysis difference in percent.

The most obvious feature is that the areas of data impact correspond to regions with TCWV amounts below 30 $kg\,m^{-2}$ due to significant cloud occurrence in moister regimes. Secondly, areas of rather systematic negative TCWV signatures appear over South Africa, the Eastern part of North Africa and, most of all, the Middle East. MERIS data tends to add humidity in the Western part of North Africa and Western Australia. Some of these signatures are still visible 3 days into the forecast and correspond to regions with rather low moisture contents and weak atmospheric dynamics.

In September 2006, the above impact has been weaker by a factor of two or so (Figure 6). From the other experiments it was found that the areas of systematic drying and moistening are quite stable between years and undergo significant seasonal variations. For illustration, Figure 7 shows the same plot for January-February 2008 (this experiment has been run with model cycle 33R2 and a static bias correction). Here, MERIS data reduces moisture in the analysis over the entire Northern part of Africa and Central Asia while significant moistening is observed just North of the ITCZ. Moisture increments in both Australia and the Middle East are negligible.

In summary, the MERIS TCWV observations produce significant regional impact that is limited to areas with little-to-moderate background moisture. It was also found that the MERIS moisture effect has little impact on cloud generation or precipitation. Note that the areas of systematic impact also match the areas with high data density shown in Figure 3c). Only little impact was noticed over the North American continent in all experiments. This could be explained with the rather well constrained moisture analysis by ground-based observations. In South America only 2007 showed some impact from MERIS data.

Figure 8 displays the analysis difference of TCWV again (as shown in Figure 5) with mean wind increments overlayed for August 2006. The humidity dipole over North Africa could suggest an enhanced East-West transport of moisture in support of the Easterly jet as well as an enhanced transport of lower level moisture from the Gulf of Guniea northwards into the ITCZ. However, mean wind differences are fairly small between

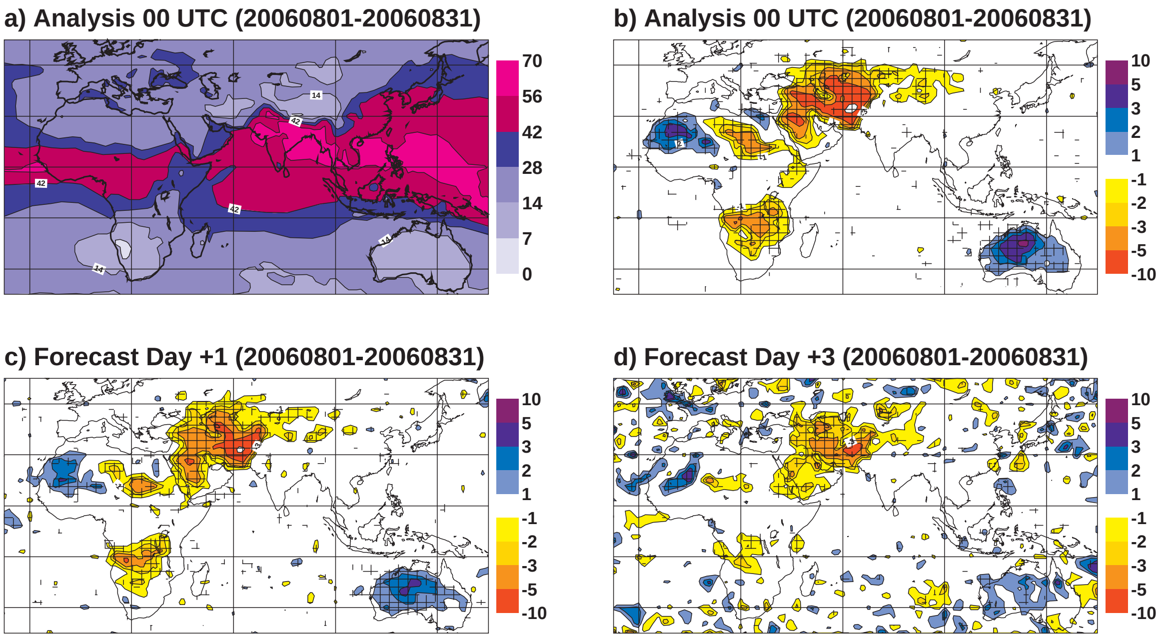

Figure 5: Mean analysis TCWV (a) and mean difference between 00 UTC analyses from experiment and control in % (b) and between forecasts for day-1 (c), and day-3 (d) for period 1-31 August 2006. Hatched areas indicate where differences are statistically significant at the 95%.

the two experiments. Given the mean intensity of the jet of 10 ms^{-1} at 600-700 hPa located at 15 degrees Northern latitude, the additional MERIS TCWV observations do not seem to affect the mid-level dynamics. At 850 hPa, some indication of additional moisture transport from the ocean can be noted but, again, the wind differences are rather small to draw a conclusion.

3.2 Performance evaluation

General observation statistics were generated from the model analyses from both MERIS and control experiments and for the special areas of interest that are listed in Table 1. These areas refer to the regions where the largest systematic impact on the moisture analysis have been noted when MERRIS observations were added to the observing system. The observation statistics were limited to radiosonde measurements of specific humidity because most other data did not show much effect. Again, only results from after the completed bias correction spin-up are shown that is August-September 2006.

Figures 9 and 10 show the fits for August 2006 and Figures 11 and 12 show the fits for September 2006. Sub-panels (a) represent the statistics for the entire set of available radiosondes while sub-panels (b) only show the statistics for Vaisala RS92 radiosondes. The reason for this distinction has been raised recently by investigations

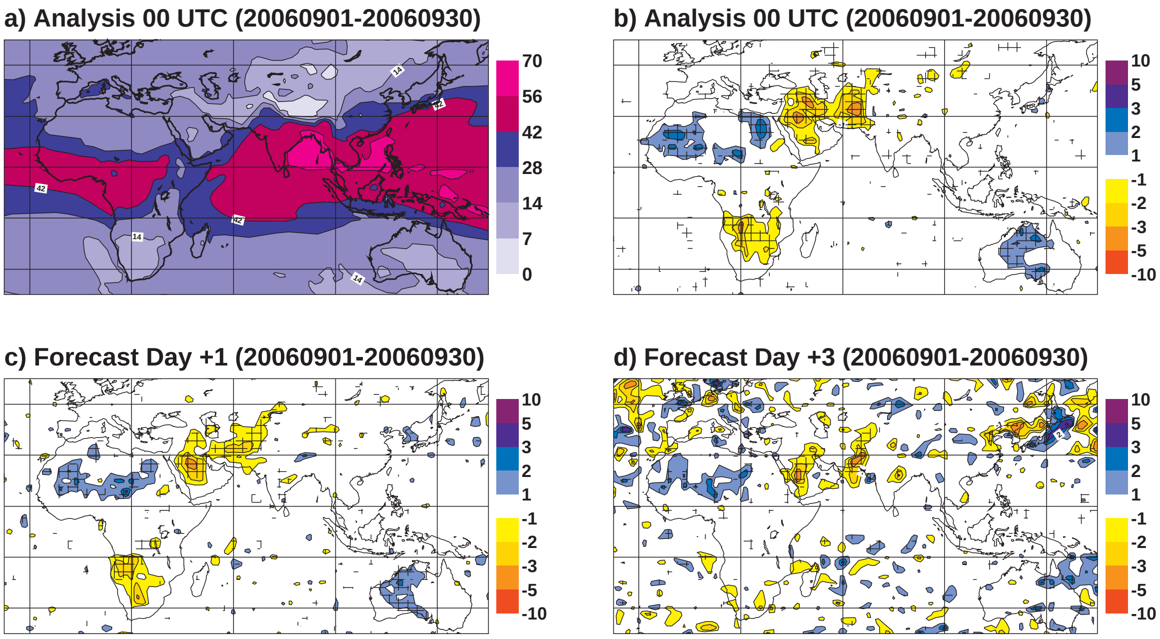

Figure 6: As Figure 5 for period 1-30 September 2006.

Table 1: Areas for which observation statistics were produced (units are degrees).

Area	min. latitude	max. latitude	min. longitude	max. longitude
Australia	-10.0	-45.0	110.0	160.0
Arabia	0.0	50.0	40.0	70.0
S.Africa	-40.0	0.0	10.0	40.0
N.Africa	10.0	35.0	-10.0	30.0
S.America	-40.0	0.0	-80.0	-30.0

related to possible (mainly dry) biases in humidity observations from radiosondes other than Vaisala RS92 in West Africa during the AMMA field campaign (Agusti-Panareda et al. 2009). These biases can be mostly related to the way humidity is measured and sonde age, the environmental temperature and moisture as well as radiative heating. Agusti-Panareda et al. found that most other sonde types exhibited dry biases between 5-30% and they developed a bias correction that is calibrated with night-time Vaisala RS92 observations and that has been verified with ground-based GPS TCWV observations.

Indeed, Figure 13 indicates that a substantial mix of radiosonde types has been used in the areas that were selected for the observation statistics over the selected areas. Even near the coast-lines of Australia and in Arabia older Vaisala sondes of the RS80-type have been deployed while over Africa and South America mostly other-than-RS92 sondes were used.

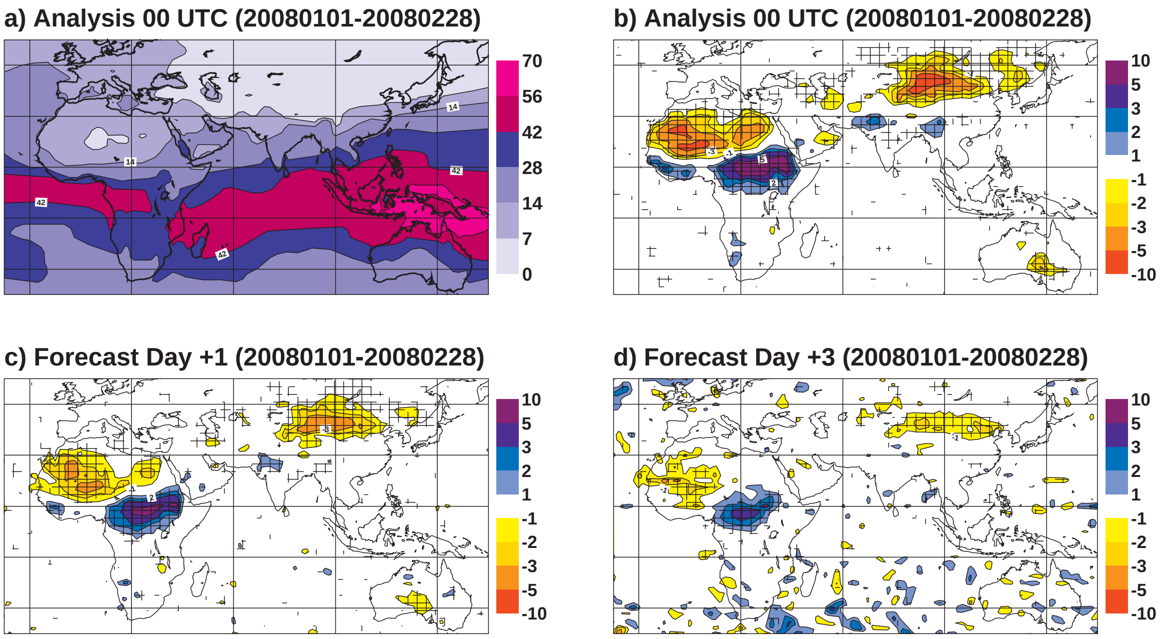

Figure 7: As Figure 5 for period 1 January - 28 February 2008.

Comparing the statistics in Figures 9a and b as well as 10a and b reveals that:

- Over *Australia* about 80% of the data is contributed by Vaisala RS92 sondes and yet observation-minus-first guess/analysis biases are entirely different between the two samples while the standard deviations are nearly identical. Since the model fields are the same in both samples, only the observations from the remaining sonde types can explain the difference. The full sample exhibits a large negative observation bias leading to negative observation-minus-model differences while the Vaisala RS92 sample exhibits a positive bias near the surface and almost no bias at levels above. The other notable feature is that the MERIS experiment performs slightly better than the control experiment with respect to RS92 sondes and much worse when all sondes are taken into account.

- Over *Arabia* the above behaviour is also shown; however, biases remain negative but are about 50% smaller for the Vaisala RS92 sample. Biases are slightly worse for the MERIS experiment while standard deviations are better.

- The statistics over *South Africa* resemble those over Arabia. Again, biases are reduced but in this case by 70%.

- Over *North Africa*, the change of both biases and MERIS experiment performance are quite large. Noticeable is that the observation-analysis biases are larger than those for the first guess from both experiments

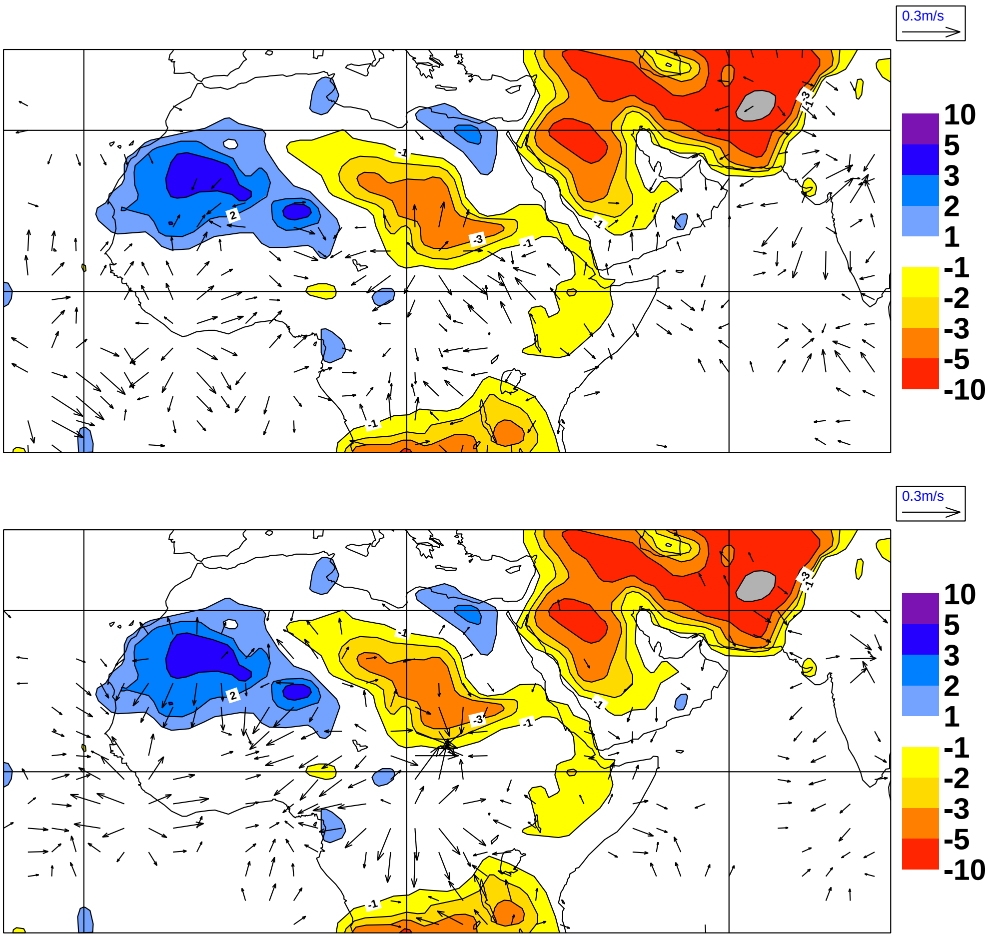

teh

Figure 8: Mean TCWV analysis difference (Meris-control, colours in %) and wind analysis difference (arrows, reference arrow length is 0.3 ms^{-1} for August 2006 at 700 hPa (top) and 850 hPa (bottom).

in the Vaisala RS92 sample. This indicates that the analysis state has been mostly driven by observations other than Vaisala RS92 and that there has been actually a real conflict between sonde observations of different kinds.

- Over *South America* the Vaisala RS92 is only 20% of the total sample but statistics are quite similar and neutral between the two experiments.

a) b)

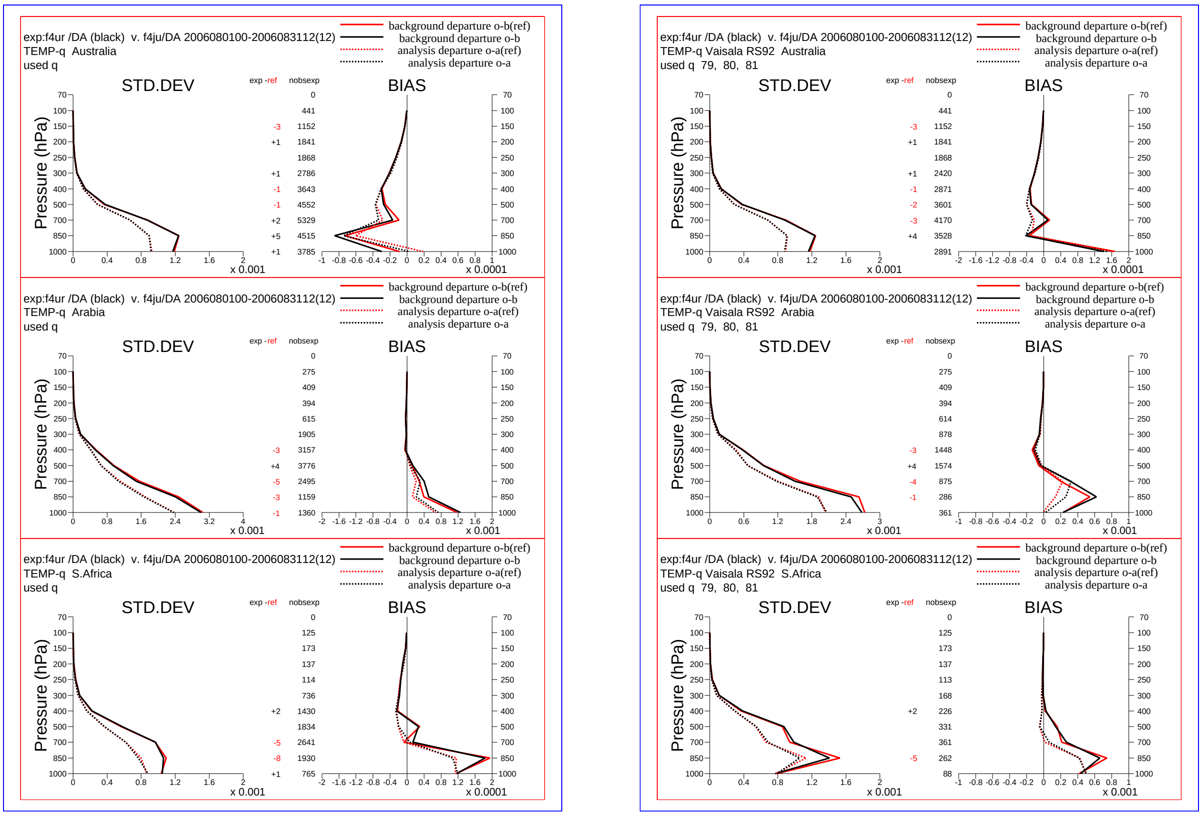

Figure 9: First-guess (solid) and analysis (dotted) fit to all (a) and Vaisala RS92 (b) radiosonde specific humidity observations over period 1-31 August 2006 for MERIS (black) and control experiments (red) in Australia (top), Arabia (middle) and South Africa (bottom).

Most of the above described features were found for both August and September (see Figure 11 and 12) and appear to represent rather fundamental features. In summary, these are the much smaller observation-model biases and much better performance of the MERIS experiment when the statistics are limited to the best available radiosonde types.

The above bias issue has been accounted for in the operational ECMWF system as of model cycle CY32R3 (Vasiljevic et al. 2007). However, only statistics from RS92 radiosonde observations have been created from 2007 onwards so that the period investigated here is still uncorrected. This explains the above significant differences in the observation statistics and further underlines the need for moisture bias correction in radiosonde data.

When forecast scores are calculated, no significant impact of the additional data can be noted in terms of moisture, wind or temperature. This is independent of the reference analysis that is used for the assessment. The most obvious explanation is that MERIS TCWV observations are only available in hours of local daylight and in cloud-free areas and that the main impact on the moisture analysis was seen in regions with little to moderate TCWV contents in the atmosphere. Only in the driest parts, this impact lasted up to a few days into the forecast mainly due to little atmospheric dynamic activity.

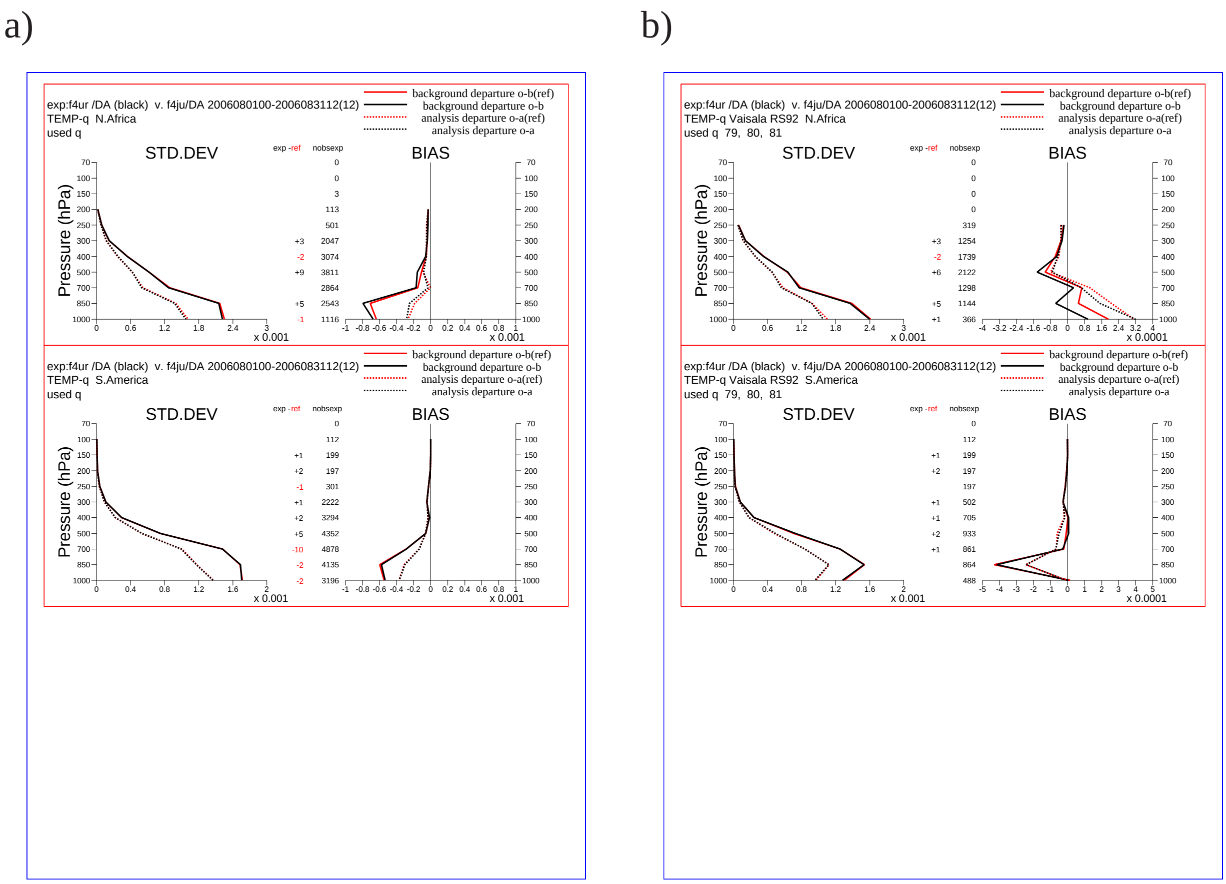

Figure 10: As Figure 9 for North Africa (top) and South America (bottom).

4 Conclusions

This paper describes the first implementation of the assimilation of total column water vapor retrievals from MERIS over land surfaces in a global and operational NWP system. The data is of rather good quality but, due to the measurement principle, only available at local daytime and in cloud-free conditions. Nonetheless, MERIS total column water vapor retrievals over land contribute an important observable that is only sparsely available from other sensors. After the lifetime of MERIS similar products from, e.g., GOME-2 onboard Metop will continue the data series so that this information source can be considered an important contribution to the moisture observing system for both operational NWP analyses and reanalysis efforts.

The impact of the data was found to be localized in arid to semi-arid regions and to produce systematic features of mean drying and moistening in North and South Africa, South America, Arabia and Australia. The mean impact on regional moisture changes with season but is rather systematic on an inter-annual basis. While the impact on mean analysis state was found to be significant, forecast scores were not significantly affected due to the lack of dynamic activity in areas with highest data density.

The evaluation of analysis impact with radiosondes showed a distinct dependence on radiosonde type. Using only Vaisala RS92 radiosondes, the impact of MERIS observations was found to be neutral to positive. If all other sonde types were included, the entire observation-model bias structures changed and revealed a negative moisture bias that has been associated with other sonde types in the past. The impact of MERIS observations was found to be negative when all sonde types were used for the evaluation, which could be interpreted such

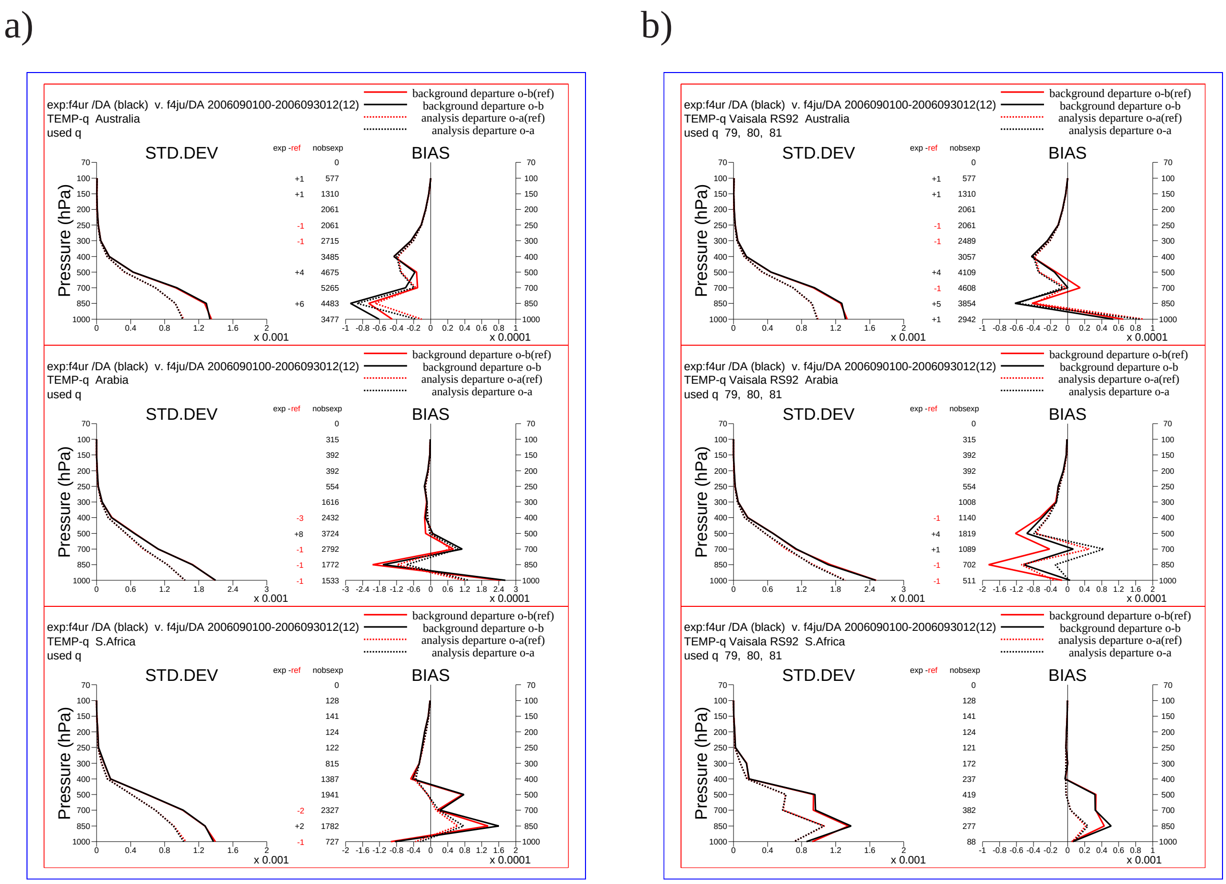

Figure 11: First-guess (solid) and analysis (dotted) fit to all (a) and Vaisala RS92 (b) radiosonde specific humidity observations over period 1-30 September 2006 for MERIS (black) and control experiments (red) in Australia (top), Arabia (middle) and South Africa (bottom).

that the MERIS observations are working against the negative sonde moisture bias.

Currently, the experiment verification is being extended by two further aspects: (1) the verification of model moisture analyses with ground-based GPS observations in West Africa over the 2006 AMMA field campaign (see also Bock et al. 2007); (2) the parallel experimentation with enhanced data usage of AMSU-B/MHS radiances over land surfaces (Karbou et al. 2009b) that seems to produce a very similar mean moisture analysis impact as was seen from the experiments in this paper. These aspects will be described in a forthcoming paper in collaboration with Météo-France.

Future developments will attempt to produce a more balanced match between observation and model fields through super-obbing to overcome the rather large discrepancy in horizontal representativeness between the two. Further, improvements to the quality control will be attempted to reduce spurious cloud contamination and it will be investigated if the bias correction scheme can be enhanced through additional bias predictores that will introduce a more adaptable air mass dependence.

Lastly, since this type of satellite observations is fairly unique over land surfaces it is important to stress (1) the requirement of near real-time availability of the latest available product version and (2) the need for data reprocessing with the latest algorithm version for NWP reanalyses to make the best use of the data over the instrument's lifetime.

a) b)

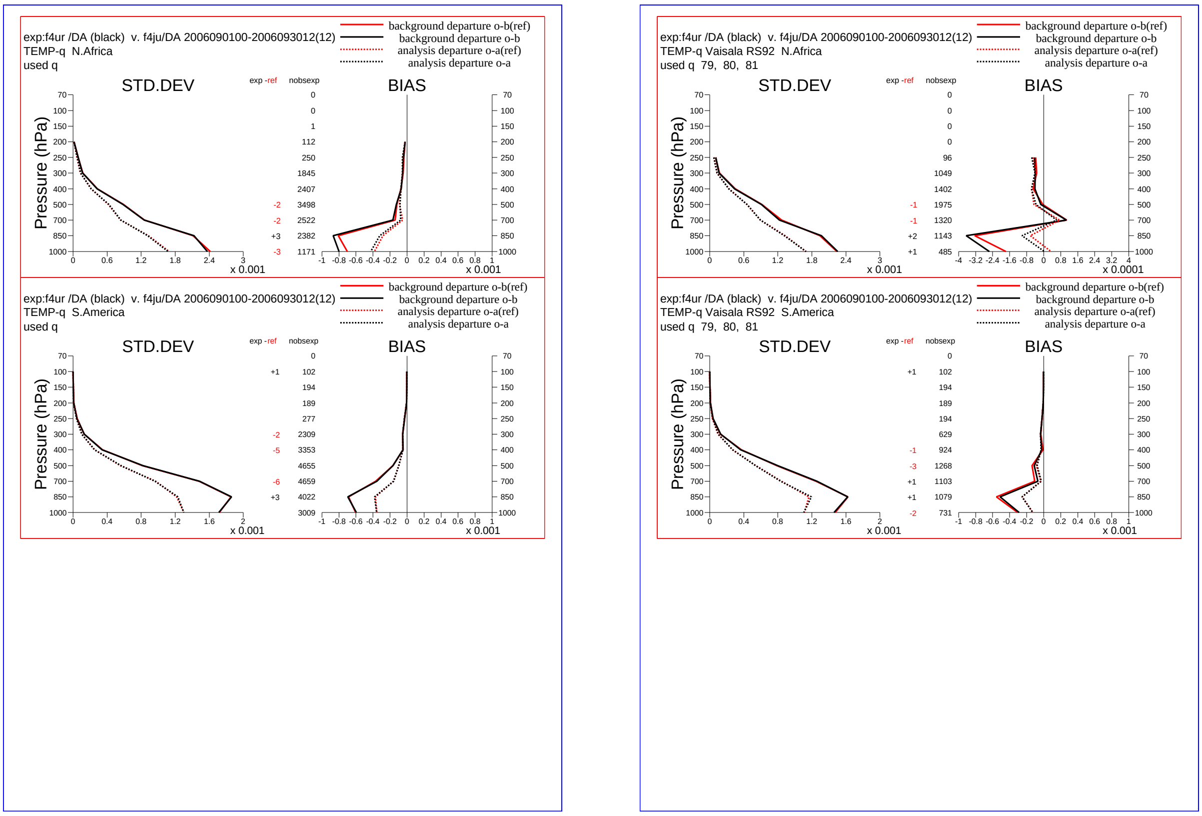

Figure 12: As Figure 11 for North Africa (top) and South America (bottom).

Acknowledgments

The author is greatly indebted to Milan Dragosavac for his help with the BUFR-data conversion, to Antonio Garcia-Mendez for supplying the radiosonde type analysis for August 2006 and to Lars Isaksen for his support with OBSTAT. The project was partly funded by the European Space Agency.

References

Abdalla, S., 2005: Global Validation of ENVISAT wind, wave and water vapour products from RA-2, MWR, ASAR and MERIS. Final report ESA contract 17585. Available from ECMWF, Shinfield Park, Reading, RG2 9AX, UK.

Agustí-Panareda, A., D. Vasiljevic, A. Beljaars, O. Bock, F. Guichard, M. Nuret, A. Garcia-Mendez, E. Andersson, P. Bechtold, A. Fink, H. Hersbach, J.-P. Lafore, J.-B. Ngamini, D.J. Parker, J.-L. Redelsperger and A.M. Tompkins, 2009: Radiosonde humidity bias correction over the West African region for special AMMA reanalysis at ECMWF. *Q. J. Roy. Meteor. Soc.*, DOI: 10.1002/qj.396.

Andersson, E., P. Bauer, A. Beljaars, F. Chevallier, E. Hólm, M. Janisková, P. Kallberg, G. Kelly, P. Lopez, A. McNally, E. Moreau, A. Simmons and J.-N. Thépaut (2005), Assimilation and modelling of the hydrological cycle. *Bull. Amer. Meteorol. Soc.*, **86**, 387-402.

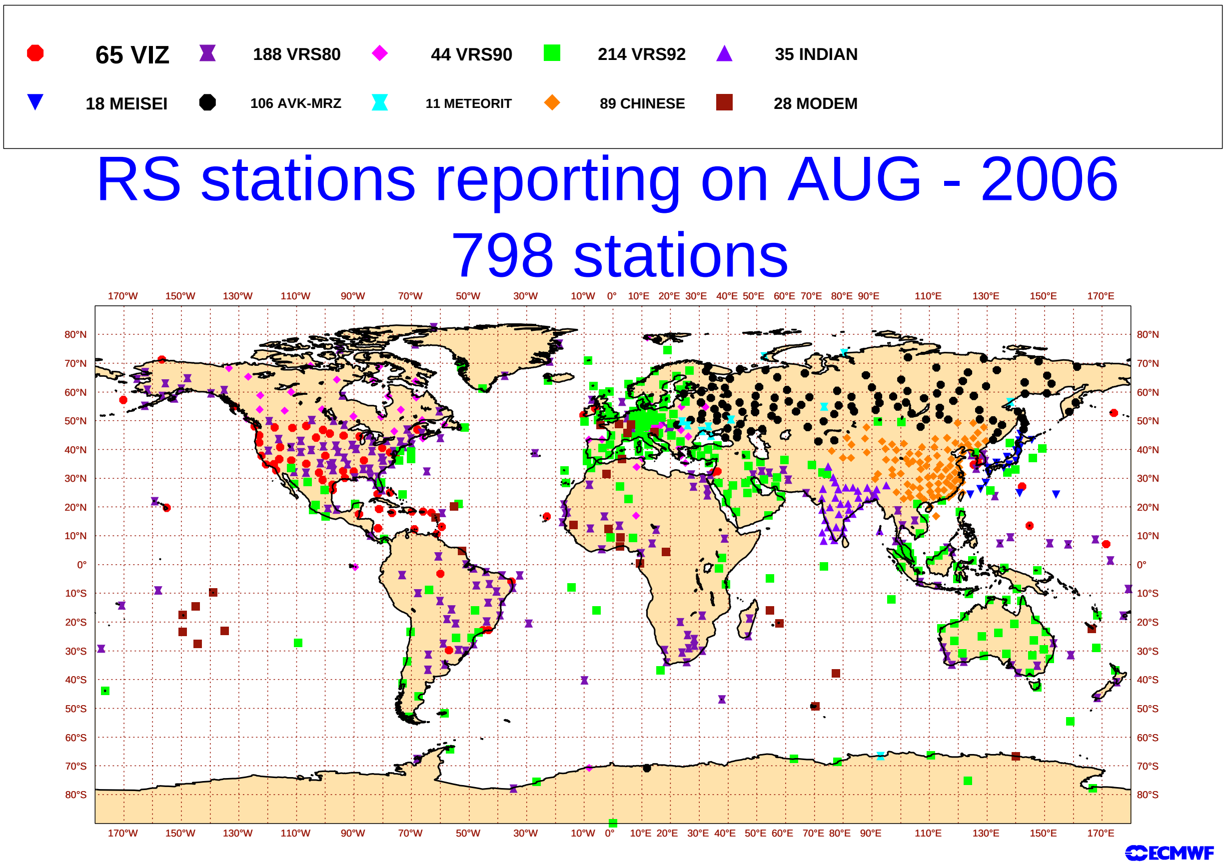

Figure 13: Radiosonde type used in the ECMWF analysis in August 2006.

Andersson, E., E. Hólm, P. Bauer, A. Beljaars, G.A. Kelly, A.P. McNally, A.J. Simmons, and J.-N. Thépaut, 2007: Analysis and forecast impact of the main humidity observing system. *Q. J. Roy. Meteor. Soc.*, DOI: 10.1002/qj.112.

Auligné, T., A.P. McNally, and D.P. Dee, 2007: Adaptive bias correction for satellite data in a numerical weather prediction system. *Q. J. Roy. Meteor. Soc.*, **133**, 631-642.

Bauer, P., P. Lopez, A. Benedetti, D. Salmond, S. Saarinen and M. Bonazzola, 2006: Implementation of 1D+4D-Var assimilation of precipitation affected microwave radiances at ECMWF, Part II: 4D-Var. *Q. J. Roy. Meteor. Soc.*, **132**, 2307-2332.

Bennartz, R., and J. Fischer, 2001: Retrieval of columnar water vapour over land from back-scattered solar radiation using the Medium Resolution Imaging Spectrometer (MERIS). *Remote Sens. Environ.*, **78**, 274-283.

Bock, O., M.-N. Bouin, A. Walpersdorf, J.-P. Lafore, S. Janicot, F. Guichard, and A. Agustí-Panareda, 2007: Comparison of ground-based GPS precipitable water vapour to independent observations and NWP model reanalysis over Africa. *Q. J. Roy. Meteor. Soc.*, DOI: 10.1002/qj.185.

Dee, D.P., 2005: Bias and data assimilation. *Q. J. Roy. Meteor. Soc.*, **131**, 3323-3343.

Hollingsworth, A., and P. Lönnberg, 1986: The statistical structure of short-range forecast errors as determined from radiosonde data. Part I: The wind field. *Tellus*,**38A**, 111-136.

Karbou, F., E. Gerard and F. Rabier, 2006: Microwave land emissivity and skin temperature for AMSU-A and AMSU-B assimilation over land. *Q. J. Roy. Meteor. Soc.*, **132**, 2333-2355.

Karbou, F., E. Gerard and F. Rabier, 2009a: Global 4D-Var assimilation and forecast experiments using land surface emissivities from AMSU-A and AMSU-B observations. Part I: Impact on sounding channels. *Q. J. Roy. Meteor. Soc.*, submitted.

Karbou, F., E. Gerard and F. Rabier, 2009b: Global 4D-Var assimilation and forecast experiments using land surface emissivities from AMSU-A and AMSU-B observations. Part II: Impact of adding surface channels on the African Monsoon during AMMA. *Q. J. Roy. Meteor. Soc.*, submitted.

Kelly, G., P. Bauer, A. Geer, P. Lopez, and J.-N. Thépaut, 2008: Impact of SSM/I observations related to moisture, clouds and precipitation on global NWP forecast skill. *Mon. Wea. Rev.*, **.136**, 2713-2726.

Krzeminski, B., N. Bormann, F. Karbou and P. Bauer, 2006: Towards a better use of AMSU over land at ECMWF. Proc. 16th International TOVS Study Conference, Angra de Reis, Brazil.

Vasiljevic, D., E. Andersson, and A. Agustí-Panareda, 2007: Radiosonde temperature and humidity bias correction for operations, research and reanalysis. ECMWF Internal Memo. R43.2/DV/0768, 19 pp.